ARTICLE IN PRESS

Ceramics International xxx (xxxx) xxx-xxx



Contents lists available at ScienceDirect

Ceramics International

journal homepage: www.elsevier.com/locate/ceramint



Phonon and phonon-related properties of MgSiN₂ and MgGeN₂ ceramics: First principles studies

Sittichain Pramchu, Atchara Punya Jaroenjittichai*, Yongyut Laosiritaworn

Department of Physics and Materials Science, Faculty of Science, Chiang Mai University, Chiang Mai 50200, Thailand

ARTICLE INFO

Keywords: DFT Phonons MgSiN₂ and MgGeN₂ Ceramics

ABSTRACTS

In this work, we used density functional perturbation theory to calculate phonon frequencies, phonon dispersions, Born effective charges, infrared (IR) absorption, and Raman spectra of $MgSiN_2$ and $MgGeN_2$. From the results, the values of phonon frequencies have the scale comparable with the values reported in the previous theoretical work. Longitudinal optical (LO) and transverse optical (TO) splitting was also included in this work. Some small alteration of phonon frequencies were then found, which is caused by LO-TO splitting at zone-center. In addition, Born effective charge calculation reveals that $MgSiN_2$ and $MgGeN_2$ have the same ionic nature compared with the previously reported $ZnSiN_2$ and $ZnGeN_2$ semiconductor. The phonon frequencies that are IR and Raman active were firstly predicted. This clarification on phonon and phonon-related properties as well as related consequences are expected to help revealing more knowledge about the nature of $MgSiN_2$ and $MgGeN_2$ in enhancing/developing the opto-electronics devices.

1. Introduction

Ultraviolet light-emitting diodes (UV-LEDs) applicable as light sources and lasers have a wide range of applications, including absorbance and fluorescence based optical measurements [1], highdensity optical data storage [2], and microelectronic fabrication technologies [3,4] etc. UV-LEDs with emission wavelengths shifted deeper into UV region of spectrum are extremely attractive or desirable. For instance, microelectronic fabrication technologies require deep UV-LEDs for improved resolution in photolithography. This therefore requires semiconductors with wide band gap for the p-n junction section of the LEDs devices. Among many wide band gap semiconductors, group III nitride compounds with wurtzite structure AlN and GaN, with band gaps at room temperature of 6.0 eV [5] and 3.4 eV [6] respectively, have been extensively researched because of their hardness, high thermal conductivity, and thermal resistance to high temperature [6]. However, there is a problem about efficiency improvement of III-N nitrides UV-LEDs i.e. the difficulty to grow highquality crystalline layers due to high lattice mismatch between the commonly used substrate sapphire (Al₂O₃) as reported in AlN/GaN case [7]. This leads to some low interface qualities and anomalous optical properties may occur. In order to deal with this problem, ternary wide band gap compounds with two different cations II-IV-N₂ such as Zn-IV-N2, where group IV elements are Si, Ge, and Sn have been intensively studied as a series analogous to III-N nitrides AlN,

GaN, and InN [8–10]. The more complex structure of II-IV- N_2 compounds allows higher degree of freedom of doping for structural and optical tuning, which opens new routes to doping-control based on defect physics. Therefore, more flexible tunability of both structural and optical properties could be achieved by considering II-IV- N_2 compounds, e.g. Zn-IV- N_2 . However, their band gap still has room for improvement, e.g. ZnSi N_2 has a band gap only of 4.46 eV [11]. Therefore, the search for new ternary semiconductors with wider band gap is still of great interest to produce the deep UV-LEDs.

Recently, there are several reports revealing that Mg-IV-N $_2$ with group IV elements as Si, Ge, and Sn has the values of band gaps higher than those from Zn-IV-N $_2$. For instance, density functional theory (DFT) calculation in Ref. [12] reports the values of 6.08 eV (indirect band gap), 5.36 eV, and 3.59 eV for MgSiN $_2$, MgGeN $_2$, and MgSnN $_2$, respectively. In addition, the results from DFT and electron energy loss spectroscopy exhibits the band gap of MgSiN $_2$ is an indirect one with the value of 6.2 eV, while the direct band gap at the Γ point is of 6.3 eV [13]. Further, Boer et al. reported the band gap of MgSiN $_2$ acquired from soft X-ray absorption and emission spectroscopy techniques is of 5.6 \pm 0.2 eV in agreement with their DFT calculated value of 5.72 eV [14]. Because of the comparable band gaps of MgSiN $_2$ and MgGeN $_2$ to those of the well-known III-N nitrides AlN, we thus focus on the investigation of MgSiN $_2$ and MgGeN $_2$ materials in this work.

Moreover, for LED applications, their efficiency (lumens per watt) of LEDs mainly rely on thermal management of LEDs device, which

E-mail address: atcharapunya@gmail.com (A.P. Jaroenjittichai).

http://dx.doi.org/10.1016/j.ceramint.2017.05.267

0272-8842/ \odot 2017 Elsevier Ltd and Techna Group S.r.l. All rights reserved.

^{*} Corresponding author.

heat generated at p-n junction has to be transferred to heat sink as fast as possible, unless the efficiency may significantly drop. Thus, the compound with high thermal conductivity is highly required, and detailed mechanism of thermal conductivity in the materials should be comprehended. Theoretically, to calculate thermal conductivity, it needs terms higher than second order term in the Taylor expansion of the crystal potential energy surface. As the second and third-order derivatives in the Taylor expansion relate to the second and third-order force constants, it is therefore convenient to consider both of them via phonon analysis. This suggests phonon calculation being important to predict a novel material for high efficiency UV-LEDs with highly effective heat transfer. Note that the phonon analysis has been widely studied for III-N compounds (e.g. AlN and GaN) [15-17] and Zn-IV-N₂ [18]. However, even Mg-IV-N₂ compounds have about 1.7 eV wider band gap than with Zn-IV-N2 compounds (e.g. MgSiN2 compared with ZnSiN₂) [11,13], there is still no report about the phonon analysis in Mg-IV-N2 groups, including the effect from LO-TO splitting. In addition, there is no report available for IR and Raman spectra as phonon related properties. Consequently, in this work, we performed density functional investigation on the phonon and phonon-related properties of Mg-IV-N2 semiconductors.

2. Materials and method

MgSiN₂ and MgGeN₂ have an orthorhombic crystal structure, which each unit cell contains 4 formula units of Mg-IV-N2 (as shown in Fig. 1). The crystal structures reported in Ref. [19] and Ref. [12] were used as initial structures in DFT calculations (structural relaxation) for MgSiN2 and MgGeN2 in this work. The calculations were performed under the framework of a plane wave method implemented in Quantum-Espresso package [20]. All pseudopotentials used here are ultrasoft from GBRV pseudopotential library [21]. The number of electrons in valence states treated in this calculation were 10, 4, 14, and 5 for Mg, Si, Ge, and N, respectively. The exchange-correlation approximation was treated under the local density approximation (LDA) with the parameters from Perdew-Zunger (PZ) [22], Energy cutoff of 60 and 720 Rydberg were found sufficiently large for wavefunctions and charge density expansion in this calculation. The k-point sampling of 6×6×6 Monkhorst-Pack [23] mesh was found to produce sufficient k-point density for phonon calculations, and were used throughout the work.

In all electronic structure calculations, the Kohn-Sham differential equations were solved iteratively using Davidson diagonalization method. The iterative procedure was terminated when the estimated energy error was less than 10^{-16} Rydberg. All crystal structures were relaxed to its minimum point of the potential energy surface using Broyden-Fletcher-Goldfarb-Shanno minimization (BFGS). The BFGS molecular dynamics cycles were executed continuously until all force and stress tensor components are less than 10^{-4} Hartree/Borh and 0.1 Kbar, respectively. Then, the acquired equilibrium structures were used in phonon calculation.

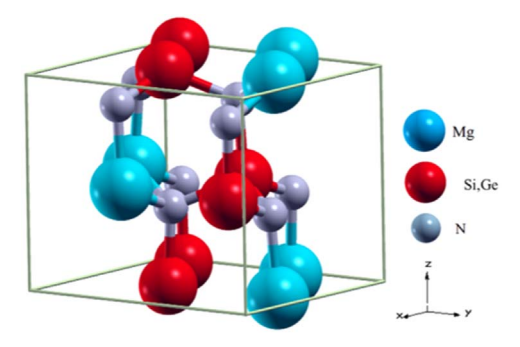


Fig. 1. Orthorhombic crystal structure of $MgSiN_2$ and $MgGeN_2$, the unit cell contains 4 formula units (16 atoms).

In condensed mater physics, phonons are generated in response to lattice vibrations. Thus, phonon properties are beyond the ground state behaviors. Thus, not only the properties based on the equilibrium structure but also the displacement perturbations of atomic positions have to be taken into account. From a theoretical point of view, an infinitesimal vibration around the equilibrium position of each atom can be created by introducing monochromatic perturbation \mathbf{u} to atomic positions $\mathbf{R}_I = \mathbf{R}_a + \mathbf{\tau}_s$, i.e.

$$\mathbf{R}_{I}[\mathbf{u}_{s}(\mathbf{q})] = \mathbf{R}_{a} + \mathbf{\tau}_{s} + \mathbf{u}_{s}(\mathbf{q})e^{i\mathbf{q}\cdot\mathbf{R}_{a}},\tag{1}$$

where, τ_s is the equilibrium position of the sth atom in the unit cell labeled by a (with vector \mathbf{R}_a). Note that the atomic displacement perturbation can probably be considered in more concise definition $\mathbf{R}_I[\Delta \tau] = \mathbf{R}_a + \tau_s + \Delta \tau$, where $\Delta \tau = \mathbf{u}_s(\mathbf{q})e^{i\mathbf{q}\cdot\mathbf{R}_a}$.

This displacement perturbation leads to a small fluctuation of total energy around a minimum of the potential energy surface (E_{tot}^0) . The total energy of a system of interest can then be expressed as [24].

$$E_{tot}(\Delta \tau) = E_{tot}^0 + \sum_{asa} \sum_{bs'\beta} \frac{1}{2} \left(\frac{\partial^2 E_{tot}}{\partial \tau_{sa}^a \partial \tau_{s'\beta}^b} \right) \Delta \tau_{sa}^a \Delta \tau_{s'\beta}^a + \cdots,$$
(2)

where $\Delta \tau_{sa}^{\alpha}$ is the displacement along direction α of the atom s from its equilibrium position τ_s . In Eq. (2), the second-order derivative of total energy with respect to atomic displacement is known as the interatomic force constants (IFCs), a fundamental quantity representing phonon characteristics of material in response to lattice displacement field. Note that Fourier transform of IFCs is connected to the dynamical matrix through

$$D_{sas,\beta}(\mathbf{q}) = \frac{1}{\sqrt{M_s M_{s,r}}} \sum_{b} \frac{\partial^2 E_{tot}}{\partial \mathbf{\tau}_{sa}^0 \partial \mathbf{\tau}_{s,\beta}^b} e^{i\mathbf{q} \cdot \mathbf{R}_b}, \tag{3}$$

where, $M_{s,(s')}$ is the atomic mass of atom s(s'). The squares of the phonon frequencies $\omega_{\bf q}^2$ at a given ${\bf q}$ are eigenvalues which can be obtained from the solution of the secular equation $\sum_{s,\beta} D_{sas,\beta}({\bf q}) {\bf u}_{s,\beta}({\bf q}) = \omega_{\bf q}^2 {\bf u}_{sa}({\bf q})$. In this work, the derivative of energy was calculated from density functional perturbation theory and linear-response approach [25,26]. The second-order derivatives of the energy versus a static electric field was investigated to extract dielectric tensors $\varepsilon_{a\beta}$, where the mixed derivatives of the static electric field and displacement was consider in obtaining the Born effective charge tensor $Z_{a\beta}^*$ [27]. The infrared (IR) intensity was calculated directly from effective charge $Z_{a\beta}^*$ and displacement pattern $U_{\beta}(b)$ via $I_{IR}(b) = \sum_{\alpha} |\sum_{s\beta} Z_{a\beta}^{*s} U_{\beta}^{s}(b)|^{2}$, where the non-resonant Raman intensity was prescribed using the Placzek's expression.

However, in order to obtain accurate phonon-related properties, one needs to impose the acoustic sum rule (ASR) based on the translational invariance of the system, where the sum of IFCs and effective charge have to be set to zero (net force on any atom and net charge of system must remain zero) [24]. In addition, to handle with the long-range Coulomb interactions which is incompatible with periodic boundary condition (because the treatment of long-range interaction requires very large supercell), a non-analytic term must be added to a force constant at ${\bf q}=0$ limit (long wavelength limit). This term depends on $Z^*_{\alpha\beta}$ and $\varepsilon_{\alpha\beta}$, which causes LO-TO splitting near gamma point [28]. For phonon dispersion, $3\times 3\times 3$ uniform distribution of ${\bf q}$ -point grid was found to give sufficiently accurate results and was used in Fourier transformation of dynamical matrix from components in k-space to force constants in real space. Phonon frequencies at high symmetry point in Brillouin zone were then calculated by inverse Fourier transforming back of these force constants.

3. Results and discussion

 $MgSiN_2$ and $MgGeN_2$ in the orthorhombic crystal structure which lattice parameters obtained from our DFT calculations are shown in Table 1. The deviation of our lattice constants and previous calculated results from the experiments are presented in the parenthesis. As

Download English Version:

https://daneshyari.com/en/article/5438865

Download Persian Version:

https://daneshyari.com/article/5438865

<u>Daneshyari.com</u>